NOVEMBER 09 2004

Propagation of sound in long enclosures

K. M. Li; K. K. lu

J. Acoust. Soc. Am. 116, 2759–2770 (2004)
https://doi.org/10.1121/1.1798351

Propagation of sound in long enclosures

K. M. Li[a] and K. K. Iu
Department of Mechanical Engineering, The Hong Kong Polytechnic University, Hung Hom, Hong Kong

(Received 21 February 2004; revised 22 July 2004; accepted 4 August 2004)

The propagation of sound in long enclosures is addressed theoretically and experimentally. In many previous studies, the image source method is frequently used. However, these early theoretical models are somewhat inadequate because the effect of multiple reflections in long enclosures is often modeled by the incoherent summation of contributions from all image sources. Ignoring the phase effect, these numerical models are unlikely to be satisfactory for use in predicting intricate patterns of interference due to contributions from each image source. In the present paper, the effect of interference is incorporated by coherently summing the contributions from the image sources. To develop a simple numerical model, the walls of long rectangular enclosures are represented by either geometrically reflecting or impedance boundaries. Measurements in a one-tenth-scale model are conducted to validate the numerical model. In some of the scale-model experiments, the enclosure walls are lined with a carpet to simulate the impedance boundary condition. It has been shown that the proposed numerical model agrees reasonably well with experimental data. [DOI: 10.1121/1.1798351]

PACS numbers: 43.20.Fn, 43.20.Mv, 43.28.Js [SFW] Pages: 2759–2770

I. INTRODUCTION

Based on the assumption of a diffuse sound field, the classic room acoustics theory has been developed and used for more than a century.[1] In long enclosures, such as corridors and tunnels, the classic formulas are unsatisfactory, as the assumption of a diffuse field does not necessarily hold due to the extreme dimensions. Kang[2] conducted measurements showing that classical room acoustics was not applicable in a long enclosure. In general, it would be rather difficult to determine the reverberant levels in a long enclosure because the sound field is inhomogeneous and the level of sound will not be constant throughout.

We note that a number of investigations relating to the reverberation in long enclosures have been carried out since the 1960s. Yamamoto[3] was among the first to study the propagation of sound in corridors. Davies[4] and Redmore[5] were also interested in the subject in the 1970s and 1980s, respectively. The ray-tracing technique and image source method were used to predict the attenuation of sound in long corridors. In the late 70s, Sergeev[6] used an image source model to derive simple formulas to estimate the propagation of sound in city streets and long tunnels. A point source was considered in his study and the total sound field was evaluated by summing contributions from all rays incoherently. However, he offered no measurement results to support his model. In the 1990s, Kang[7,8] proposed theoretical expressions derived from the image source method to calculate reverberation times in long rectangular rooms with geometrically reflecting walls. In the late 1990s, Imaizumi *et al.*[9] used a conical beam method, which combined the advantages of the ray-tracing technique and the image source method, to predict the propagation of sound along a ''T''-shaped tunnel. In a recent study, Yang and Shield[10] developed a ray-tracing computer model for the detailed investigation of sound fields in long enclosures.

The effects of interference due to multiple reflections of sound rays from boundary walls were generally ignored in all of the previous studies mentioned above. It is important to point out that in the late 70s Gensane and Santon[11] considered the wave nature of sound in their study of sound fields in bounded and arbitrarily shaped spaces. Lemire and Nicolas[12] extended this approach by using a spherical-wave reflection coefficient instead of a plane-wave reflection coefficient to model the propagation of waves in a bounded space. In particular, they investigated the sound fields in a rectangular enclosure and in the region bounded by two infinite parallel planes. Their predicted results agreed very well with the standard normal-mode solutions, but no experimental validations were presented. It is also notable that the Acoustical Society of Japan published a simple numerical scheme to predict the propagation of road traffic noise in tunnels.[13] This numerical scheme is referred as the ASJ model in the following discussions and analysis.

The current study is motivated by the need to reduce the levels of noise inside a road traffic tunnel. A simple yet accurate model for prediction is required to assess the propagation of sound in tunnels with absorptive lining. In this paper, we wish to investigate the propagation of sound in long enclosures both theoretically and experimentally. A numerical scheme is developed using a complex image source theory according to Lemire and Nicolas.[12] Scale-model experiments are conducted to validate their theory. This preliminary study will provide a basis for assessing the propagation of sound in tunnels.

In Sec. II, we describe three models frequently used to model the propagation of sound in long enclosures: the incoherent model, the complex image source model (also known as the coherent model), and the ASJ model. Section III presents experimental results as well as theoretical predictions

[a]Electronic mail: mmkmli@polyu.edu.hk

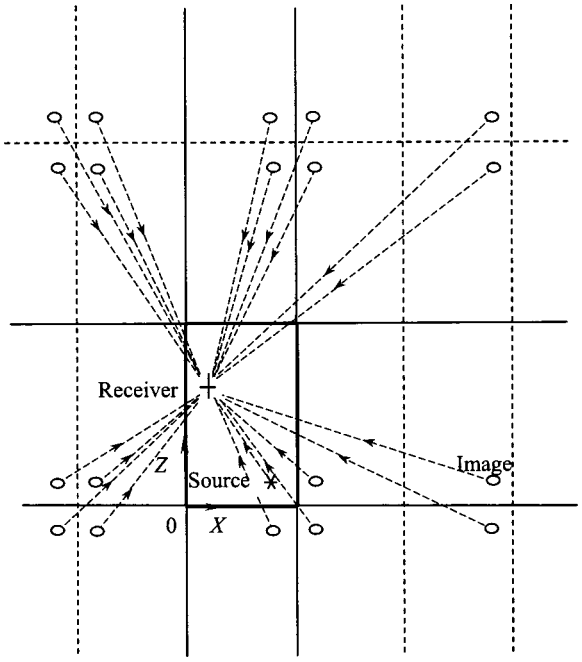

FIG. 1. Rows of image sources formed in a tunnel by reflections of four boundaries.

according to coherent and incoherent models for various impedance boundary conditions. Finally, conclusions are drawn in Sec. IV.

II. THEORETICAL MODELS

A. Ray model—Incoherent summation

In studying the effects of interference due to the direct ray and its reflected rays from the boundaries of long enclosures, the propagation model reviewed here was based on a typical case of rectangular long enclosures with geometrically reflecting boundaries (see Fig. 1). Diffusion is ignored and the absorption coefficient of the boundaries is assumed to be independent of the incident angle.

According to the acoustic ray models developed by Yamamoto[3] in the 1960s, by Davies[4] in the 1970s, by Redmore[5] in the 1980s, and by Kang[2] in the 1990s, the sound field at a particular receiver position is considered to be a summation of the intensities from the direct and each image source. Taking into consideration the absorption of the boundaries, the total intensity, I, can be obtained by incoherently summing all contributory components to yield

$$I = I_{\mathrm{ref}} d_{\mathrm{ref}}^2 \sum_N \frac{R_N}{d_N^2}, \tag{1}$$

where I_{ref} is the free-field sound intensity of the source at a reference distance of d_{ref} from the source, d_N is the length of the path from the image source to the receiver, and R_N is the reflection factor which represents the fraction of sound energy reflected from the boundaries. We remark that the attenuation due to the absorption of sound in air has been ignored in Eq. (1). The path length d_N can be determined in a straightforward manner by simple geometrical considerations. The reflection coefficient for each interaction with a boundary surface is simply given by

$$R_N = 1 - \alpha_j, \tag{2}$$

where α_j $(j=1,2,3,4)$ is the respective absorption coefficients of the walls of the rectangular enclosure. The reflection factor R_N is the combined reflection coefficient associated with the image source n. The amplitude of R_N is reduced by a factor $(1-\alpha_j)$ for each interaction with the corresponding boundary surface. An implicit assumption of the model given in Eq. (1) is that the mutual effects of the interference of direct and all reflected waves are ignored. We refer to this model as the incoherent model.

The absorption coefficients of the boundaries of long enclosures vary from case to case depending on the surface finish. Kang,[8] and Yang and Shield[10] conducted field measurements in an underground station, the surfaces along the length of which were all of concrete. They assumed in their models that the absorption coefficients of all boundaries were the same, ranging from 0.03 to 0.07 at octave bands of 125 to 4000 Hz. In our study, these parameters for absorption coefficients are used in our subsequent numerical analyses, unless otherwise stated.

B. Complex image source theory—Coherent model

Although the wave nature of sound fields in enclosed spaces was studied by Gensane and Santon,[11] and by Lemire and Nicolas,[12] they presented no experimental validations of their theoretical formulations. In a recent study, Dance *et al.*[14] have developed an interference model for calculating the total sound fields in an industrial space. However, their model is only accurate at receivers located close to the reflecting surfaces. We plan to explore these earlier models both theoretically and experimentally to investigate the effect of finite impedance on the overall sound fields in a long enclosure.

In previous publications, Iu and Li[15] derived an expression for the propagation of sound in a narrow city street. Lemire and Nicolas[12] formulated a solution for the propagation of sound in a bounded space. These two theoretical models are based on an analytic Green's function that was also a complex image source model. A spherical wave reflection coefficient was included in their numerical models to account for the reflection from the surface of an impedance boundary. In the current study, we follow Lemire and Nicolas in representing a long enclosure using two parallel vertical inwalls of infinite extent and two parallel horizontal planes, namely, the ground and ceiling. The width of the long enclosure is W, with the left vertical wall located at a plane of $x=0$. The height of the long enclosure is H, with the ground situated at a plane of $z=0$. Both the ground and ceiling are assumed to be perpendicular to the vertical walls. The schematic diagram in Fig. 1 shows a view of the plan of the posed problem, and illustrates formation of the first- and second-order image sources. The source and receiver are located at $(x_s,0,z_s)$ and (x,y,z), respectively. As the sound field is symmetrical at about the $y=0$ plane, we are interested in the region where $x \in [0,W]$, $y \in [0,\infty)$, and $z \in [0,H]$.

As can be seen from Fig. 1, the total sound field is composed of contributions from the direct source, and a series of image sources is produced by reflections of the two parallel walls from the source located at $(x_s,0,z_s)$. In addition, the total sound field is augmented by infinite rows of image sources due to the presence of a reflecting ceiling and the reflecting ground. The total sound field due to a monopole of unit strength can be computed by summing all contributions coherently to yield

$$P=\frac{1}{4\pi}\sum_{N=0}^{\infty} Q_{sN}\frac{e^{ikd_N}}{d_N}, \tag{3}$$

where d_N is the distance of the image source n and the receiver, and Q_{sN} is the combined complex wave reflection coefficient associated with the image source n. At each interaction with a boundary plane, the complex wave reflection coefficient, Q_N, is determined according to[16]

$$Q_N \equiv Q(d_N,\beta_i,\theta_N)=R_p+(1-R_p)F(w_N), \tag{4}$$

with the plane-wave reflection coefficient, R_p, given by

$$R_p=\frac{\cos\theta_N-\beta_j}{\cos\theta_N+\beta_j}, \tag{5}$$

where θ_N is the incident angle of the reflected wave of the image source n, and β_j ($j=1$, 2, 3, and 4 for the four boundary surfaces of the long enclosure) is the specific normalized admittance of the corresponding boundary surface. The term $F(w_N)$ is known as the boundary loss factor, which can be determined by

$$F(w_N)=1+i\sqrt{\pi}w_N e^{-w_N^2}\,\mathrm{erfc}(-iw_N), \tag{6}$$

with the parameter w, which is also known as the numerical distance, defined by

$$w_N=\sqrt{kd_N/2}(1+i)(\cos\theta_N+\beta_j). \tag{7}$$

The successive reflections of a spherical wave due to an image source n are then modeled by the product of the spherical wave reflection coefficient Q_N pertaining to each reflection in the sequence. This product, the overall complex wave-reflection coefficient, is labeled as Q_{sN} in Eq. (3). As pointed out by Lemire and Nicolas, Eq. (3) represents a first-order approximate solution, but Allen and Berkeley[17] have shown that this solution is an exact one when all of the boundary walls are rigid, i.e., $\beta_j=0$ and hence $Q_{sN}=1$. In this case, the solution can be written simply as

$$P=\frac{1}{4\pi}\sum_{n=0}^{\infty}\frac{e^{ikd_N}}{d_N}. \tag{8}$$

Hodgson *et al.*[18] revealed that the introduction of porous absorbers into a scale model of a factory led to unexpected effects. He found that the absorptive effect of boundaries was dependent on the shape of the enclosure and could not be measured in the usual way in a reverberation chamber. Recently, Kang[19] studied the effect of architectural acoustic treatments to improve the intelligibility of speech in a long enclosure. He pointed out that the attenuation of sound along the length of the enclosure is greater when the sound absorbers are along three or four boundaries rather than along one or two. However, at present, there is no validated theoretical model that takes into account the effects of mutual interference from all image sources for predicting the propagation of sound in a long enclosure with impedance boundary conditions.

C. The ASJ prediction model

The Research Committee on Road Traffic Noise of the Acoustical Society of Japan published a Prediction Model 1998 for Road Traffic.[13] Hereafter, we refer to this numerical scheme as the ASJ model. The model is used to predict the propagation of road traffic noise in tunnels. It is based on a sound energy balance inside the tunnel. Numerically, it is a simple model for the calculation of noise radiation in the tunnels, as two imaginary sources are assumed in the model. The first imaginary source represents the direct sound field in the tunnel. The residual sound field due to the effect of multiple reflections between the tunnel walls is calculated by the second imaginary source, which represents a distribution of surface sources.

The ASJ model was adopted by Kobayashi *et al.*[20] to predict noise propagation in a road tunnel. Attenuation at the straight and curved sections of the tunnel showed similar reduction characteristics, with a reduction rate of 4 dB per doubling of distance, up to a distance of 250 m. It was observed that the measured data over a distance of 300 m showed a greater reduction than predicted. The effect due to air absorption was ignored in the ASJ model.

Although the predicted tunnel attenuation agreed quite well with the experimental data, the measured decay rates at the 63-Hz and 125-Hz octave bands were rather irregular: no clear attenuation was observed. Kobayashi *et al.* indicated that this was possibly due to mode resonance at particular sections of the tunnel, or reflections at the open ends of the tunnel.

Tachibana *et al.*[21] carried out experimental measurements in a 1:40 scale-model tunnel to validate the ASJ model. Their experimental results showed that the propagation of sound was dependent on the source frequency. They concluded that the ASJ model could only be used as a first-order approximation for estimating the noise attenuation in tunnels.

In a recent study, Takagi *et al.*[22] demonstrated that the ASJ model was a simple and useful numerical scheme applicable to the prediction of road traffic noise in tunnels. To predict the road traffic noise in tunnels of a rectangular cross section, they derived a simple expression for the attenuation of sound energy as follows:

$$I=I_{\mathrm{ref}}\frac{2d_{\mathrm{ref}}^2}{wH}\tan^{-1}\left(\frac{wH}{\sqrt{(\alpha_t d)^4+(w^2+H^2)(\alpha_t d)^2}}\right), \tag{9}$$

where I is the predicted sound intensity at a horizontal distance d from the source, I_{ref} is the reference sound intensity at a reference distance of d_{ref} from the source in the free-field condition, H is the height of the tunnel, and $2w$ is the width of the tunnel. The absorption parameter, α_t is an empirical factor used to account for the acoustical characteristics of the tunnel walls. It vanishes when the tunnel has a perfectly

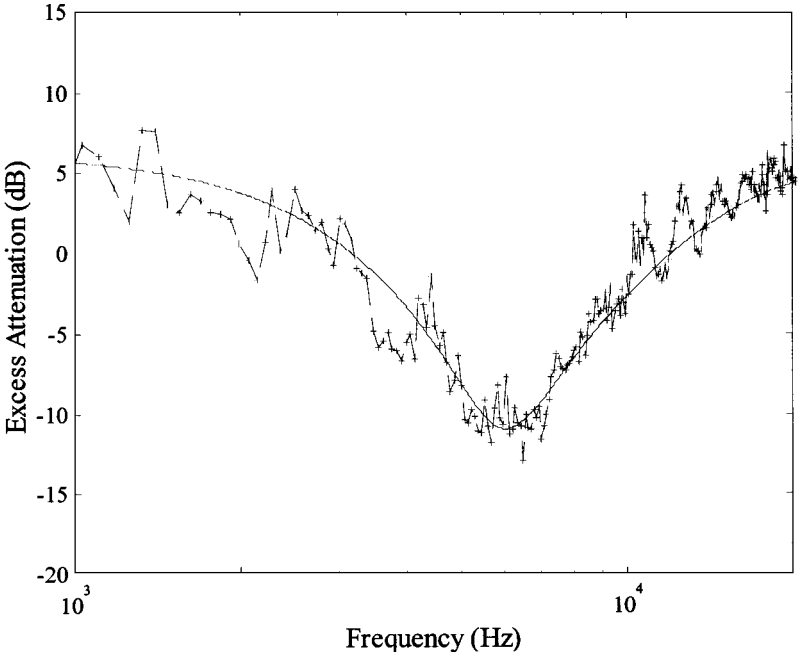

FIG. 2. Characterization of the impedance of a carpet. Both source and receiver are 0.065 m above the ground and are separated from each other at 1.0 m. (Measurement: dashed line with crosses; Theoretical prediction: solid line).

reflecting boundary. The absorption parameter was normally obtained by experimental measurements and a value of 0.04 was determined for the concrete walls.[22] Takagi *et al.*[22] proposed an empirical formula for the determination of α_t as follows:

$$1-\alpha_t=(1-\alpha)^{0.48}, \tag{10}$$

where α is the sound absorption coefficient of the material.

It is worth pointing out that the ASJ model offers a simpler formula than the incoherent model proposed by Redmore[5] and Kang[7] for predicting the sound field. Results of sound measurements in a highway tunnel showed good agreement with the ASJ model where discrepancies of less than 2 dB were reported between measured data and predictions.[22]

III. NUMERICAL SIMULATIONS AND EXPERIMENTAL RESULTS

A. Numerical simulations

The total sound field is composed of contributions from the direct source and from a series of image sources produced by multiple reflections of the two parallel walls due to the source located at $(x_s,0,z_s)$. In addition, the total sound field is also augmented by infinite rows of image sources due to the presence of a reflecting ceiling on the top and a ground surface on the bottom. The total sound field can be estimated by summing up the contributions from each of these sources.

In the presentation of numerical and experimental results, we use the term excess attenuation (EA). EA is defined as the ratio of the total sound field at various receiver locations, P, to the free-field sound pressure at 1 m from the source. Thus, EA is given by

$$\mathrm{EA}=20\log(P). \tag{11}$$

On the other hand, a comparable definition is needed for the excess attenuation if the incoherent model is used to predict the sound fields. In this case, the excess attenuation can be defined as the ratio of the total intensity level, I, to the free-field intensity level measured at 1 m from the source. It is simply given by

$$\mathrm{EA}=10\log(I), \tag{12}$$

where the total intensity level can be obtained from Eq. (1).

B. Scale-model experiments

To study the sound field in nondiffuse spaces, Hodgson *et al.*[18] used a 1:50 scale model to investigate factory sound fields with considerable success. However, it was found that the introduction of porous absorbers into the model resulted in unexpected effects. In the 1990s, Orlowski[23] built a model of an existing factory at a scale of 1:16. Comparisons of the measurements of field and scale models showed good agreement. In the late 90s, Orlowski[24] used scale modeling to study the intelligibility of speech in underground stations. Tachibana *et al.*[21] used a 1:40 scale model to predict the radiation of sound from the mouths of tunnels. Kang[25] developed a computer model to predict the temporal and spatial distribution of train noise in underground stations. In his study, a 1:16 scale physical model was constructed to validate the prediction model. To compensate for the effect of the absorption of air at high frequencies, measurements were carried out in a test tunnel filled with oxygen-free nitrogen at a concentration of 97% to 99%.

In the present study, a larger model tunnel at a scale of one-tenth was built for our experimental measurements. Experimental data were obtained to validate the theoretical models described in Sec. II. In fact, the use of a larger scale in the construction of a model tunnel proved to be a relatively simple and inexpensive technique, because the measurements can be carried out in normal atmospheric conditions without the need to fill the test tunnel with oxygen-free nitrogen. Sandwich-type steel panels 60 mm thick were used to build the model long duct with acoustically hard boundaries. The outer skin of the panel was made of 1.5-mm-thick

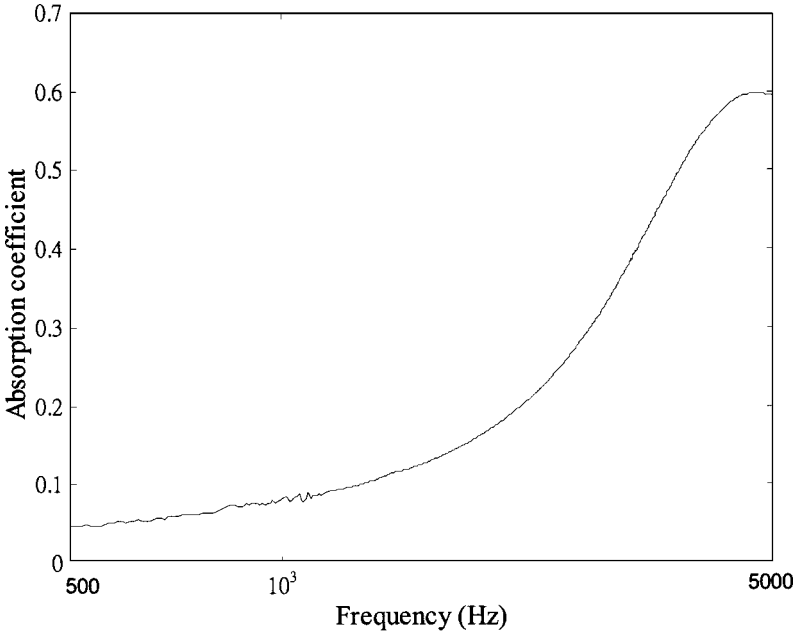

FIG. 3. The normal incidence absorption coefficient of the carpet measured using the impedance tube method.

galvanized steel sheet and the infill with 50-mm-thick fiberglass. To minimize the effects of vibration from the galvanized steel sheet, a 9-mm-thick gypsum board was stuck to the inside surface of the steel sheet. Due to the size of the model long duct, all measurements were conducted in an open space in a factory. During our measurements, the level of background noise was monitored to ensure that it was always below 60 dB, with typical signal levels inside the model long duct well above 75 dB. This precautionary step was necessary for all experimental measurements to minimize any effects from the background.

The steel panels were assembled to have an internal width and height of 1.0 and 0.6 m, respectively. To prevent the sound waves from reflecting back into the model long duct due to the effect of end reflection, an anechoic termination was designed according to ISO 7235-1996.[26] The anechoic termination was erected at the end of the test duct on the receiving side for all experimental measurements. The overall length of the model long duct was 8.5 m. At full scale, the model represents a cross section of a rectangular tunnel 10 m in width and 6 m in height. In the following paragraphs, we refer to all dimensions as scaled distances unless otherwise stated.

A Brüel & Kjær 1/2-in. condenser microphone and a Tannoy driver were used as a receiver and a point source, respectively. A PC-based maximum length sequence system analyzer (MLSSA)[27] was used both as a signal generator for the source and as an analyzer for the subsequent processing of data. The maximum length sequence (MLS) technique was chosen in the present study because Vörlander *et al.*[28] had confirmed the validity of applying MLS techniques to measure sound in highly reverberant sound fields. Indeed, the MLS technique was also chosen by Kang[8] to carry out his site measurements in an underground train station with a tunnel having a dimension of 20 m in width, 5.7 m in height, and 200 m in length.

In the current study, the MLS technique has the advantage that no correction of background noise is necessary for a signal-to-noise ratio of 0 dB. As MLSSA was operated in the time domain where the impulse response was measured, the chosen data for processing were based on the time between the arrival of the direct and the last order rays. The time-series data were converted to spectral data by the fast Fourier transform (FFT) technique. Each spectrum level was then normalized by the prerecorded direct field measurement taken at 1 m from the source at the free field. The final output was then the required excess attenuation spectrum.

In addition to hard duct walls, some measurements were conducted to model conditions when the boundary walls were covered with sound absorption materials. Carpets were fixed on one or both vertical panels of the model duct and were used to simulate a soft wall surface. Prior experiments were performed to characterize the acoustic impedance of the carpet at the open space of the factory. The MLS technique was again used for the characterization, with both the source and receiver set at a height of 0.065 m above the carpet and

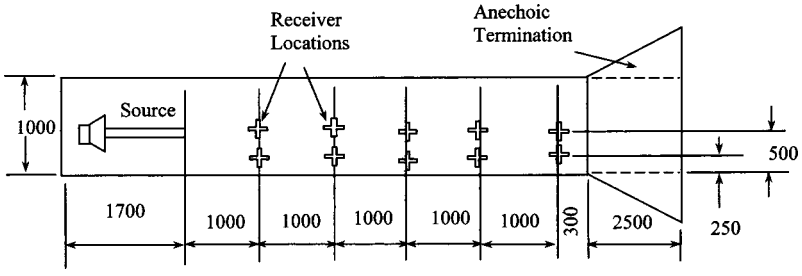

FIG. 4. The schematic sketch illustrates the model tunnel with anechoic termination.

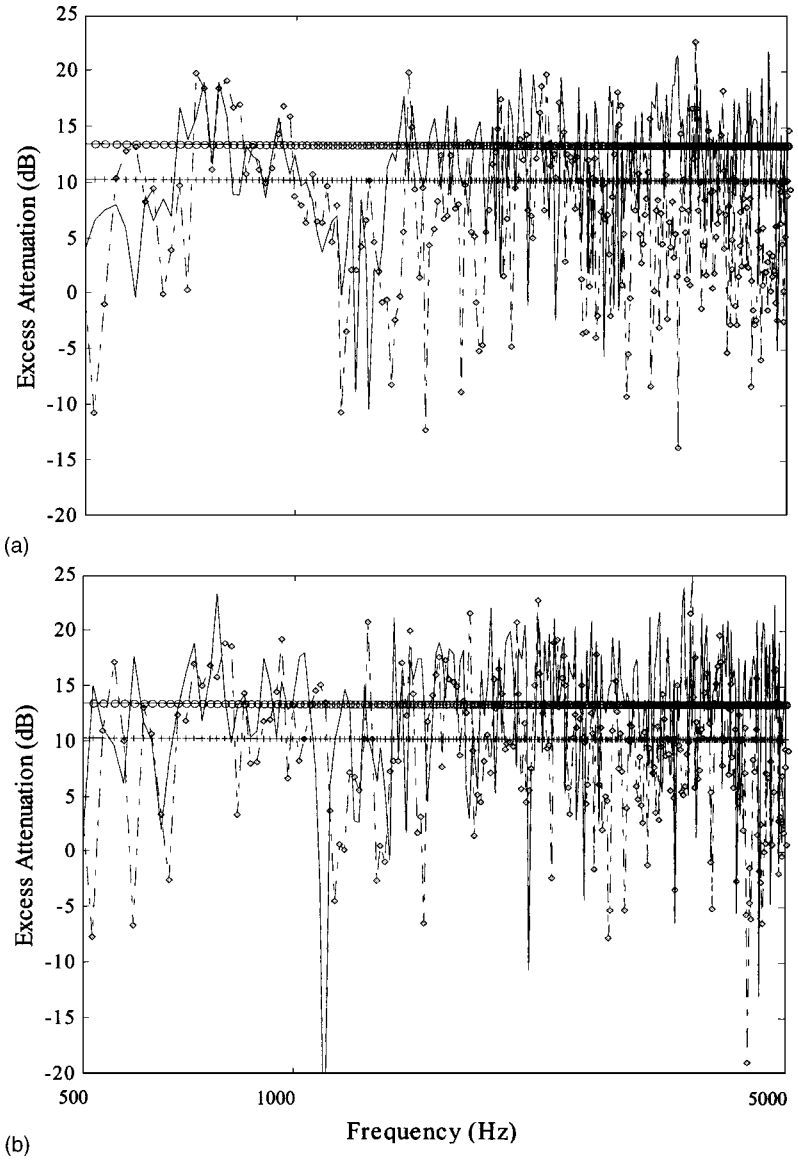

FIG. 5. Comparison of the measured spectrum of excess attenuation with the respective predictions by the coherent, incoherent, and ASJ models. Measurements were conducted in a model tunnel with hard boundaries. Both the source and receiver were located at 0.11 m above the ground. The source/receiver geometries are as follows: (a) source at (0.5,0,0.11) and receiver at (0.25,5,0.11), and (b) source at (0.25,0,0.11) and receiver at (0.25,5,0.11) (Measurement: dashed-dotted line with closed circles; Coherent prediction: solid line; Incoherent prediction: solid line with open circles; dotted line with crosses).

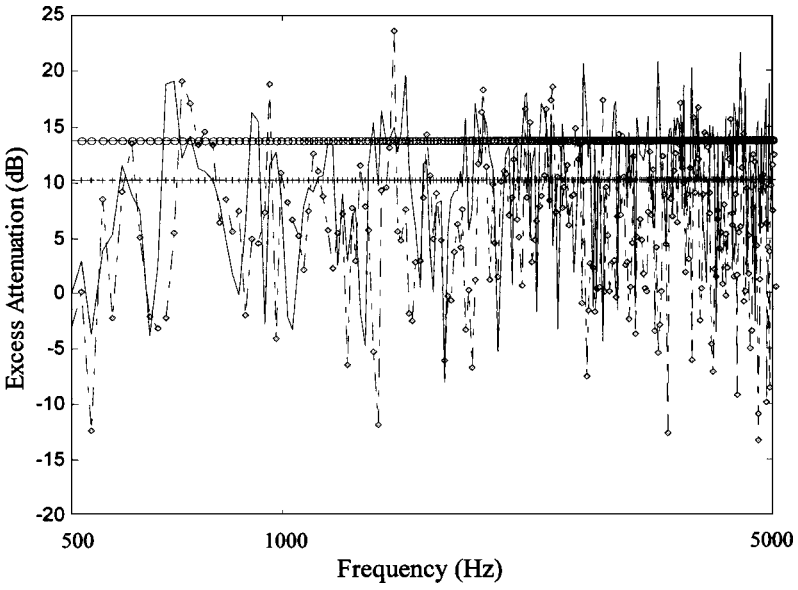

FIG. 6. Comparison of the measured spectrum of excess attenuation with the respective predictions by the coherent, incoherent, and ASJ models. Measurements were conducted in a model tunnel with hard boundaries. The source and receiver are located at different heights of 0.11 and 0.3 m, respectively. In addition, the source is situated at the centerline and the receiver at the offset line. They are separated by a horizontal distance of 4 m. The key of this figure is same as Fig. 5.

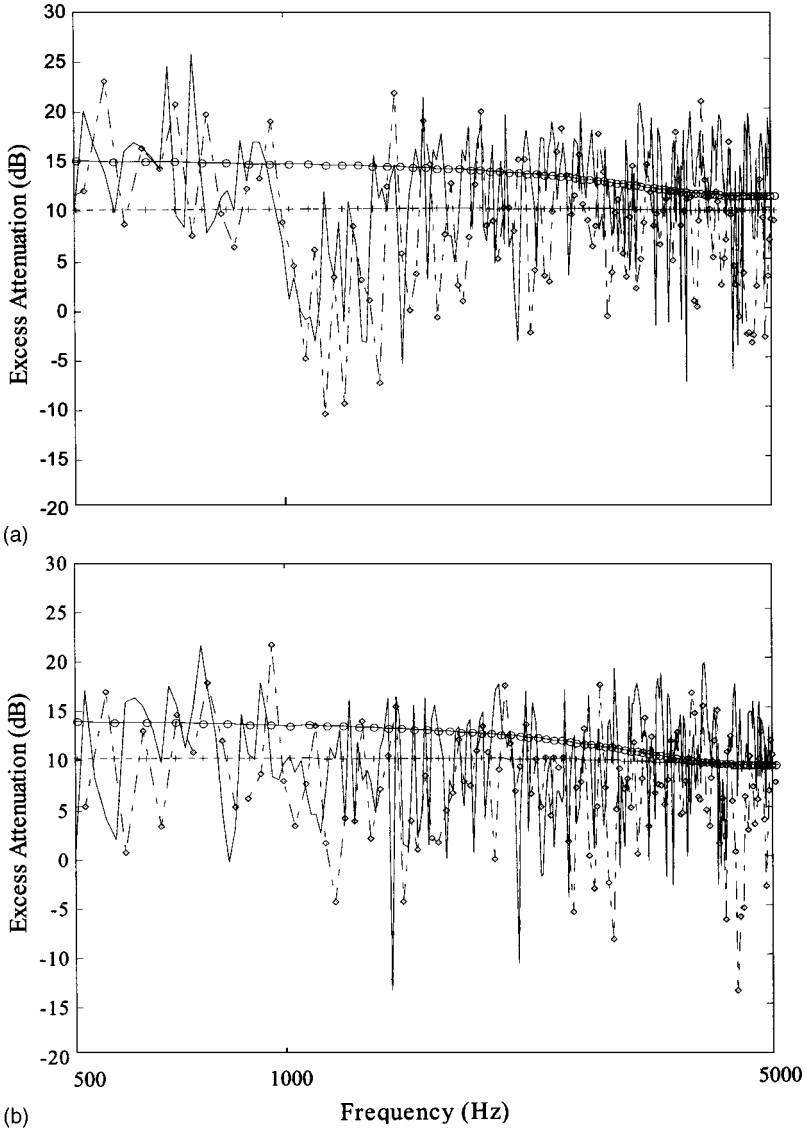

FIG. 7. Comparison of the measured spectrum of excess attenuation with the respective predictions by the coherent, incoherent, and ASJ models. Measurements were conducted in a model tunnel with an impedance wall and both the source and receiver were located at the offset line. The key of this figure is same as Fig. 5. The source/receiver geometries are as follows: source at (0.25,0,0.11) and receiver at (0.25,1,0.11); (b) source at (0.25,0,0.11) and receiver at (0.25,2,0.11).

their horizontal separation set at between 0.5 and 1.0 m.

A two-parameter model,[29] with respective best-fit parameter values for the effective flow resistivity σ_e and the effective rate of change of porosity with depth α_e of 250 kPa s m^{-2} and 300 m^{-1}, was used to calculate the impedance. A typical measurement of the excess attenuation spectrum with the horizontal separation set at 1 m was shown in Fig. 2. In the same figure, we also show the numerical predictions indicating a reasonably good fit with the experimental data for the given parameter values.

While the impedance characterized by the two-parameter model is used in the coherent ray model, an absorption coefficient at a normal incidence is used in the incoherent model. It is determined by means of the impedance tube method according to ASTM C384-98,[30] where the data acquisition system includes a Brüel & Kjær two-microphone impedance measurement tube type 4206, a power amplifier type 2706, two 1/4-in. microphones type 4187 with preamplifiers, a data acquisition front-end type 2827, and a personal computer with pulse software. Figure 3 shows the measured absorption coefficients versus the frequency. The measured absorption coefficient, α, of the carpet used in the experimental measurements varies from 0.05 to 0.6 at frequencies ranging from 500 to 5000 Hz.

The excess attenuation was measured experimentally at various receiver locations, with the source located 0.11 m above the ground. The height of the source was chosen to simulate the approximate locations of noise emitted from heavy vehicles at about 1.1 m (full scale) above the surface of tunnel roads. The source and receiver were located either at the centerline or on the side of the tunnel 0.25 m away from the centerline. In all measurements, the receivers were located at heights of either 0.11 or 0.3 m from the ground. The horizontal distances between the source and receivers ranged from 1 to 5 m (see Fig. 4 for the monitoring stations of the experimental setup).

In the numerical simulations, we can show that 30 to 50 reflections are generally required to give satisfactory results in this model long enclosure. The final choice of the number of reflections is dependent on the boundary condition of the enclosure and the source/receiver geometry. The path length from the 50th image sources to the receiver corresponds to about 30 m in our scale-model measurement. The absorption of sound in air was not significant at such a path length and

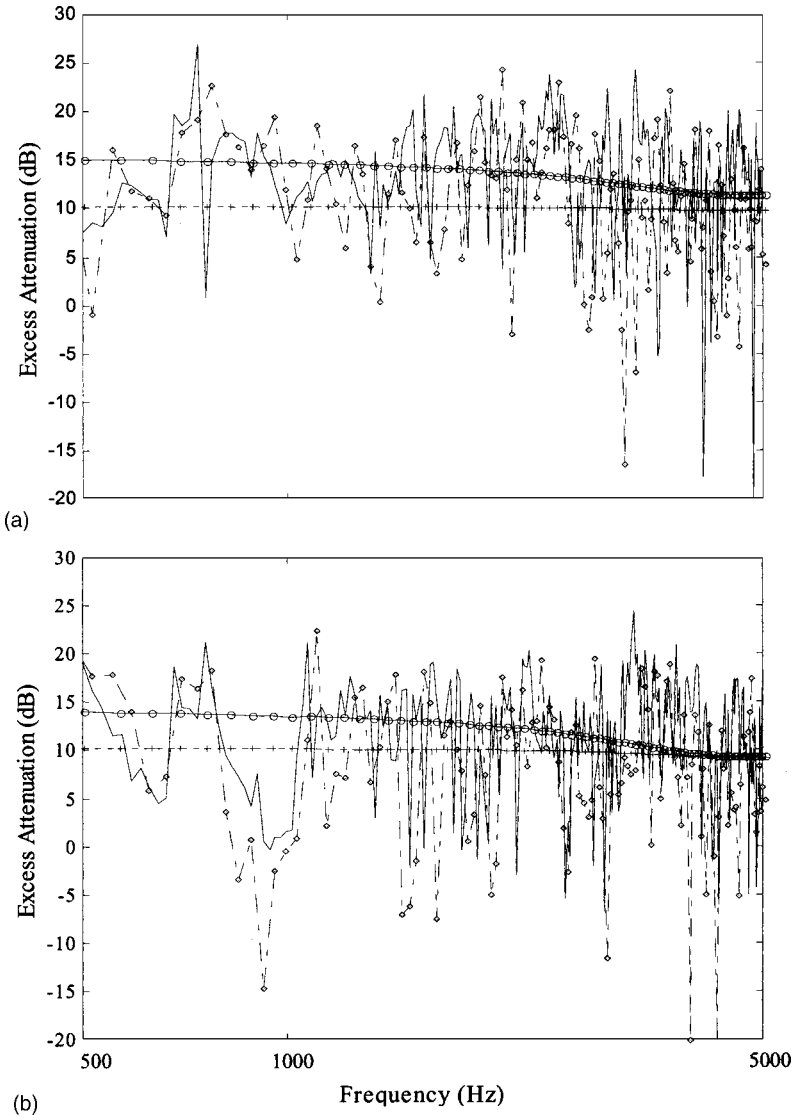

FIG. 8. Comparison of the measured spectrum of excess attenuation with the respective predictions by the coherent, incoherent, and ASJ models. Measurements were conducted in a model tunnel with an impedance wall and both the source and receiver were located at the centerline. The key of this figure is same as Fig. 5. The source/receiver geometries are as follows: (a) source at (0.5,0,0.11) and receiver at (0.5,1,0.11), and (b) source at (0.5,0,0.11) and receiver at (0.5,2,0.11).

at frequencies up to 10 kHz; hence, its effect was not included in our analyses.

1. Validations in the model tunnel with hard boundaries

To demonstrate the effect of mutual interference, the receiver was placed at the offset line and at a height of 0.11 m. Measurements were taken at a horizontal distance of 5 m in front of the source, which was also located at a height of 0.11 m above the ground. In the measurements, the source was placed at either the centerline or at the offset line located 0.25 m from the centerline. Figures 5(a) and (b) show the experimental results for the source located at the centerline and the offset line, respectively. The measured excess attenuation spectra fluctuate considerably as the source frequency increases. In Fig. 5(a), there is a distinct ''dip'' that occurs at a frequency of around 1250 Hz (125 Hz at full scale), while Fig. 5(b) illustrates no destructive interference effect occurs at the same frequency. The measured excess attenuations around 1250 Hz shown in Fig. 5(b) are increased by more than 5 dB when comparing with Fig. 5(a). In the same figure, predictions according to the incoherent model and ASJ model are also shown. We note that predictions by the incoherent model and ASJ model are only based on the path lengths between the source and receiver. Consequently, the same prediction of EA was obtained across the whole spectrum in Figs. 5(a) and (b). As shown in the comparisons, only the predictions by the coherent model give good agreements with the measurements. The incoherent model and ASJ model cannot predict such fluctuations in frequency. The results predicted by the incoherent model and ASJ model are independent of the frequency of sound and do not give good agreements with the measurements.

The pattern of the fluctuation in frequency spectrum is dependent on the relative positions of source and receiver. To illustrate this point, another measurement was taken with the source and receiver located at respective heights of 0.11 m and 0.3 m above the ground. The horizontal separation between the source and receiver was reduced to 4 m in this set of measurements. During the measurement, the source was situated at the centerline and the receiver at the offset line. In the measured results shown in Fig. 6, several distinct dips occur at frequency below 1000 Hz (100 Hz at full scale). The pattern of fluctuation in the frequency spectrum is quite different from that shown in Figs. 5(a) and (b).

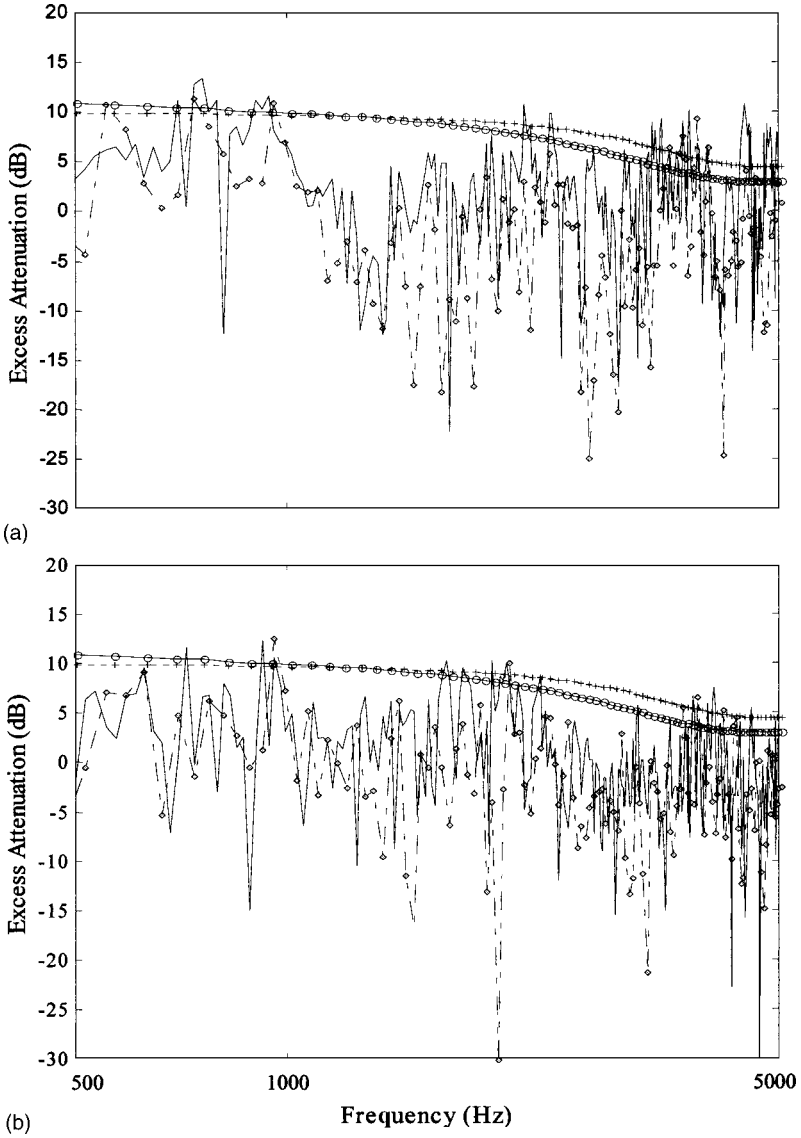

FIG. 9. Comparison of the measured spectrum of excess attenuation with the respective predictions by the coherent, incoherent, and ASJ models. Measurements were conducted in a model tunnel with two impedance walls and the receiver was located at the offset line. The key of this figure is same as Fig. 5. The source/receiver geometries are as follows: (a) source at (0.5,0,0.11) and receiver at (0.25,5,0.11), and (b) source at (0.25,0,0.11) and receiver at (0.25,5,0.3).

The effect of interference was also found when both the source and receiver were situated at other locations. These results were shown elsewhere,[31] and not repeated here. Again, only the predictions using the coherent model agree reasonably well with the measurements. The incoherent and ASJ models can only give an indication of the average levels of noise. These two models tend to give a better agreement in the average noise levels with measured results at frequencies higher than about 3000 Hz for the typical geometry used in the present study. However, the incoherent and ASJ models are unable to predict variations with frequency because they ignore the effects of the interference from all contributing rays.

2. Validations in the model tunnel with an impedance wall surface

The effect of mutual interference also occurs in tunnels with an impedance wall surface. Figure 7(a) illustrates that a distinct dip occurs at around 1100 Hz (110 Hz at full scale) when the receiver is located 1 m directly in front of and at the same height as the source. When the receiver is moved to a distance of 2 m in Fig. 7(b), the effect of destructive interference becomes less significant. We note that only the results of the prediction by the coherent model agree reasonably well with the measurements, while the incoherent model and ASJ model give an approximate mean value of the excess attenuations across the frequency spectra. In Figs. 7(a) and (b), both the source and receiver are located at the offset line close to the impedance wall. If the source and receiver are moved to the centerline, by locating the receiver at 1 m directly in front of and at the same height as the source, the dip at 1100 Hz disappears as shown in Fig. 8(a). Apparently, it seems that the impedance wall will reduce the levels of sound if both the source and receiver are located close to the impedance wall. However, by locating the receiver 2 m directly in front of and at the same height as the source at the centerline, Fig. 8(b) shows that there a distinct dip at around 900 Hz (90 Hz at full scale) while Fig. 7(b) displays a peak there. This shows that there is no simple relationship between the position of the impedance wall and the location of the source–receiver when predicting sound fields in long tunnels.

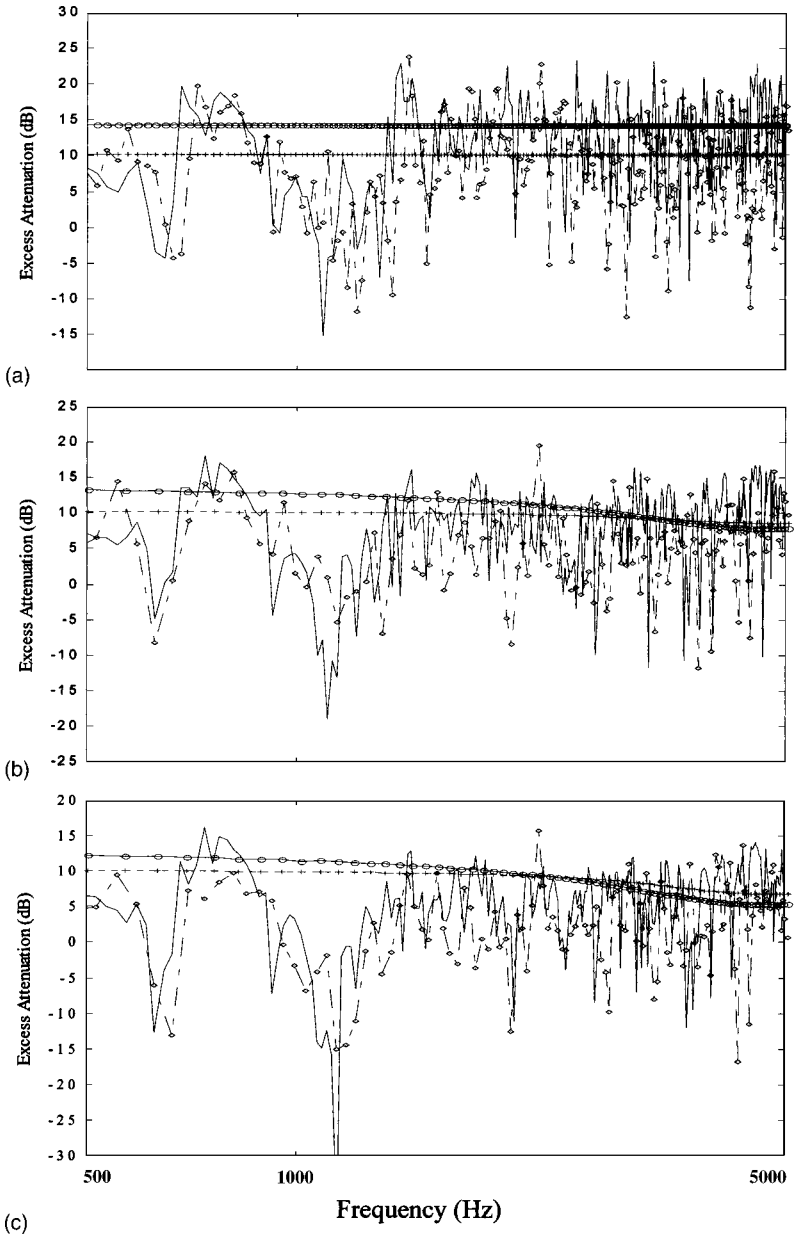

FIG. 10. Comparison of the measured spectrum of excess attenuation with the respective predictions by the coherent, incoherent, and ASJ models. Measurements were conducted in a model tunnel with different boundary conditions. The source was located at (0.25,0,0.11) and receiver at (0.5,3,0.11). The key of this figure is same as Fig. 5. The source/receiver geometries are as follows: (a) hard boundaries (no impedance wall); (b) one impedance wall; and (c) two impedance walls.

3. Validations in a model tunnel with two impedance wall surfaces

The coherent model can be used to predict the peaks and dips of the interference in the tunnel with impedance wall surfaces. The usefulness of the coherent model for predicting the sound field in a tunnel with an impedance wall has been demonstrated in the last section. Here, we extend the study to cover the situation where there are two parallel impedance wall surfaces in the long enclosure. To compare the numerical and experimental results, the predicted excess attenuations, together with the measured excess attenuations, are plotted against the frequency. Figures 9(a) and (b) illustrate two typical examples for the receiver located at the offset position and at a horizontal distance of 5 m from the source. Figure 9(a) displays the experimental results where both the source and receiver were located at 0.11 m above the ground but the source was located at the centerline. On the other hand, the configuration for Fig. 9(b) was the same as Fig. 9(a) except that the source was located at the offset line. Again, good agreements between the theoretical predictions by the coherent model and experimental measurements are evident from the results as shown in these two figures. We reiterate that the most important point to note is that the coherent model can well predict the general trend of the experimental data in the frequency spectrum, while the incoherent and ASJ models tend to give higher estimated excess attenuations and cannot predict the fluctuations in frequency caused by the effects of interference.

It is increasingly common to install sound absorption panels onto wall surfaces in tunnels to reduce the noise from traffic.[32] In this section, we explore the effects of adding an impedance wall or two parallel impedance walls in a tunnel with a stationary source, a point monopole source at a height of 0.11 m (1.1 m at full scale) above the ground. Figures 10(a)–(c) show the effect of the impedance wall on the level of sound produced by the source located at the offset line, which is 0.25 m away from the centerline of the tunnel. The receiver is located 0.11 m above the ground at the centerline

and at a horizontal distance of 3 m from the source. The impedance wall leads to decreased values in the levels of sound throughout the whole frequency range. Figures 10(a)–(c) compare the levels of sound in tunnels with reflecting hard surfaces, one impedance wall, and two impedance walls. By introducing an impedance wall, sound levels are reduced by about 3 dB across the whole frequency spectrum being displayed. By adding another impedance wall, the levels of sound are further reduced by about 2 to 3 dB.

In general, the theoretical predictions by the coherent model agree reasonably well with the measurements using experimental scale model. This suggests that the effect of interference should not be ignored when predicting the propagation of sound along tunnels. Although the measurements are conducted for a frequency range of 0.5 to 10 kHz (50 to 1000 Hz at full scale), for the sake of clarity all of the figures displayed are from 500 to 5000 Hz. We also wish to point out that the spectra of the excess attenuation are presented in the current study. These measured results allow detailed comparisons of experimental data with the numerical models in a more precise manner. The investigation of sound attenuation in octave bands in tunnels is a subject of future studies.

IV. CONCLUSIONS

In this paper, three prediction schemes, the coherent, incoherent, and ASJ models, were presented to predict the propagation of sound in long enclosures. The incoherent and ASJ models were based on a summation of the intensities from the direct and image sources without taking into account the effect of mutual interference. The coherent model, on the other hand, included the effects of the interference caused by the direct and reflected waves in the computation of sound fields. The total sound field was calculated by coherently summing the contributions from all image sources. An extensive set of one-tenth scale-model experiments were conducted in frequencies ranging from 500 to 5000 Hz and at a horizontal distance of up to 5 m in a model tunnel with a cross-sectional area of 1×0.6 m. It was shown that the theoretical predictions by the coherent model agree reasonably well with the results of the measurement, with an accuracy in most cases of well within 3 dB. However, the incoherent and ASJ models give less satisfactory agreement with the experimental measurements and their predictions are not able to match the peaks and dips caused by the effects of interference in the frequency spectra. They are only capable of predicting average noise levels at the high-frequency regime where the overall effect of multiple reflections becomes more significant. It is interesting to note that, as expected, the introduction of impedance walls resulted in a considerable increase in the attenuation of sound in the long enclosure.

ACKNOWLEDGMENTS

One of the authors (K.K.I.) was supported by a Teaching Company Scheme jointly sponsored by the Industry Department of the HKSAR Government and NAP Acoustics (Far East) Limited. The research described in this paper was supported by the Research Grants Council of the HKSAR Government and The Hong Kong Polytechnic University. The authors are grateful to NAP Acoustics (Far East) Limited for the provision of the model long duct.

[1] W. C. Sabine, *Collected papers on Acoustics* (Harvard University Press, Cambridge, MA, 1927).
[2] J. Kang, ''The unsuitability of the classic acoustical theory in long enclosures,'' Architect. Sci. Rev. **39**, 89–94 (1996).
[3] T. Yamamoto, ''On the distribution of sound in a corridor,'' J. Acoust. Soc. Jpn. **17**, 286–292 (1961).
[4] H. G. Davies, ''Noise propagation in corridors,'' J. Acoust. Soc. Am. **53**, 1253 (1973).
[5] T. L. Redmore, ''A theoretical analysis and experimental study of the behavior of sound in corridors,'' Appl. Acoust. **15**, 161–170 (1982).
[6] M. V. Sergeev, ''Scattered sound and reverberation on city streets and in tunnels,'' Sov. Phys. Acoust. **25**(3), (1979).
[7] J. Kang, ''Reverberation in rectangular long enclosures with geometrically reflecting boundaries,'' Acustica **82**, 509–516 (1996).
[8] J. Kang, ''A method for predicting acoustic indices in long enclosures,'' Appl. Acoust. **51**, 169–180 (1997).
[9] H. Imaizumi, S. Kunimatsu, and T. Isei, ''Sound propagation and speech transmission in a branching underground tunnel,'' J. Acoust. Soc. Am. **108**(2), 632–642 (2000).
[10] L. Yang and B. M. Shield, ''The prediction of speech intelligibility in underground stations of rectangular cross section,'' J. Acoust. Soc. Am. **109**(1), 266–273 (2001).
[11] M. Gensane and F. Santon, ''Prediction of sound fields in rooms of arbitrary shape: The validity of the image sources method,'' J. Sound Vib. **63**, 97–108 (1979).
[12] G. Lemire and J. Nicolas, ''Aerial propagation of spherical sound waves in bounded spaces,'' J. Acoust. Soc. Am. **86**, 1845–1853 (1989).
[13] Research Committee of Road Traffic Noise in Acoustical Society of Japan, ''ASJ Prediction Model 1998 for Road Traffic Noise,'' J. Acoust. Soc. Jpn. **55**(4), 281–324 (1999).
[14] S. M. Dance, J. P. Roberts, and B. M. Shield, ''Computer prediction of sound distribution in enclosed spaces using an interference pressure model,'' Appl. Acoust. **44**, 53–65 (1995).
[15] K. K. Iu and K. M. Li, ''The propagation of sound in narrow street canyons,'' J. Acoust. Soc. Am. **112**(2), 537–550 (2002).
[16] T. F. W. Embleton, ''Tutorial on sound propagation outdoors,'' J. Acoust. Soc. Am. **100**, 31–48 (1996).
[17] J. B. Allen and D. A. Berkeley, ''Image method for efficient simulating small-room acoustics,'' J. Acoust. Soc. Am. **65**, 943–950 (1979).
[18] M. R. Hodgson and R. J. Orlowski, ''Acoustic scale modeling of factories. II. 1:50 scale model investigations of factory sound fields,'' J. Sound Vib. **113**, 257–271 (1986).
[19] J. Kang, ''Scale modeling for improving the speech intelligibility from multiple loudspeakers in long enclosures by architectural acoustic treatments,'' Acustica **84**, 689–700 (1998).
[20] Y. Kobayashi, S. Seki, T. Kitamura, K. Mitsui, and S. Yamada, ''Study on the characteristics of noise propagation in tunnel and noise control with absorbing material of ceramics,'' Proc. Internoise **99**, 517–522 (1999).
[21] H. Tachibana, S. Sakamoto, and A. Nakai, ''Scale model experiment on sound radiation from tunnel mouth,'' Proc. Internoise **99**, 387–392 (1999).
[22] K. Takagi, T. Miyake, K. Yamamoto, and H. Tachibana, ''Prediction of road traffic noise around tunnel mouth,'' Proc. InterNoise **2000**, 3099–3104 (2000).
[23] R. J. Orlowski, ''Scale modeling for predicting noise propagation in factories,'' Appl. Acoust. **31**, 147–171 (1990).
[24] R. J. Orlowski, ''Underground station scale modeling for speech intelligibility prediction,'' Proc. Inst. Acoust. **16**, 167–172 (1994).
[25] J. Kang, ''Modeling of train noise in underground stations,'' J. Sound Vib. **195**(2), 241–255 (1996).
[26] British Standard BS EN ISO 7235, ''Acoustics—Measurement procedures for ducted silencers—Insertion loss, flow noise and total pressure loss,'' pp. 21–25 (1996).
[27] D. D. Rife and J. Van der Kooy, ''Transfer-function measurement with maximum-length sequences,'' J. Audio Eng. Soc. **37**(6), 419–443 (1989).
[28] M. Vorlander and M. Kob, ''Practical aspect of MLS measurements in building acoustics,'' Appl. Acoust. **52**(3/4), 239–258 (1997).

[29] K. Attenborough, ''Ground parameter information for propagation modeling,'' J. Acoust. Soc. Am. **92**, 418–427 (1992).
[30] ASTM Standard C384, ''Standard test method for impedance and absorption of acoustical materials by the impedance tube method,'' (1998).
[31] K. K. Iu, ''The prediction of noise propagation in street canyons and tunnels,'' M. Phil. thesis, The Hong Kong Polytechnic University (2003).
[32] H. Woehner, ''Sound propagation at tunnel openings,'' Noise Control Eng. J. **39**(2), 47–56 (1992).